Pirani Vacuum Gauges Using Silicon-on-Glass and Dissolved-Wafer Processes for the Characterization of MEMS Vacuum Packaging

Ebru Sagiroglu Topalli, Kagan Topalli, *Member, IEEE*, Said Emre Alper, Tulay Serin, and Tayfun Akin, *Member, IEEE*

***Abstract*—This paper presents the design and implementation of Pirani vacuum gauges for the characterization of vacuum packaging of microelectromechanical systems (MEMS). Various Pirani vacuum gauges are fabricated with two different standard in-house fabrication processes, namely the silicon-on-glass (SOG) process and dissolved-wafer process (DWP). The Pirani gauges utilize meander-shaped suspended silicon coils as the heaters and two isolated silicon islands in the close proximity of the heater that function as dual-heat sinks to enhance the sensitivity and dynamic range as compared to a microbridge with a single heat sink. The gauges are designed to occupy an area of 4 mm $\times$ 1.5 mm. The DWP Pirani gauge fabricated with a structural thickness of 14 μm and a gap of 2 μm shows a measured sensitivity of 4.2×10^4 (K/W)/Torr in a dynamic range of 10–2000 mTorr. The SOG Pirani gauge fabricated with a structural thickness of 100 μm and a gap of 3 μm shows a lower measured sensitivity of 3.8×10^3 (K/W)/Torr in a dynamic range of 50–5000 mTorr; however, the 100 μm-thick structural layer results in a much more robust process against stress-based deformations in suspended silicon compared to the DWP Pirani gauges. Each gauge is used to monitor the pressure of a different packaging approach. The DWP Pirani gauge is used to detect the pressure of a wafer-level vacuum package, where the pressure inside the cavity is measured to be about 2.4 mTorr. The SOG Pirani gauge is used the monitor the pressure inside a hybrid platform package which is vacuum-sealed using a projection welder, where the pressure is measured to be about 1400 mTorr. These measurements verify that the DWP and SOG Pirani gauges can be used for the characterization of wafer-level or hybrid platform vacuum packages for MEMS devices.**

***Index Terms*—Microelectromechanical systems (MEMS), packaging, Pirani gauge, pressure sensor, vacuum.**

Manuscript received June 02, 2008; revised August 12, 2008; accepted August 12, 2008. Current version published February 13, 2009. This research is supported by The Scientific and Technical Research Council of Turkey (TUBITAK) and Turkish State Planning Organization (DPT). The associate editor coordinating the review of this paper and approving it for publication was Dr. Subhas Mukhopadhyay.

E. S. Topalli is with the Department of Electrical and Electronics Engineering, Middle East Technical University, 06531 Ankara, Turkey and also with the Department of Engineering Physics, Ankara University, 06100 Ankara, Turkey (e-mail: etopalli@metu.edu.tr).

K. Topalli, S. E. Alper, and T. Akin are with Department of Electrical and Electronics Engineering and METU-MEMS Center, Middle East Technical University, 06531 Ankara Turkey (e-mail: kagan@metu.edu.tr; said@metu.edu.tr; tayfuna@metu.edu.tr).

T. Serin is with Department of Engineering Physics, Ankara University, 06100 Ankara, Turkey (e-mail: serin@eng.ankara.edu.tr).

Color versions of one or more of the figures in this paper are available online at http://ieeexplore.ieee.org.

Digital Object Identifier 10.1109/JSEN.2008.2012200

I. Introduction

HERMETICALLY sealed vacuum packaging of microelectromechanical systems (MEMS) is essential for nertial sensors like gyroscopes, optical devices, and some radio frequency (RF) MEMS structures. MEMS devices can either be packaged individually after dicing the MEMS wafer or at the wafer-level prior to dicing in order to reduce the cost [1]–[3]. For both of the packaging approaches, it is important to monitor the pressures inside the package after the initial packaging and after long-term operation. Long-term stability and *in situ* measurement of the pressures of the traditional vacuum-sealed hybrid platform packages are evaluated using Helium leak rate and Q-factor extraction techniques [3], [4]. However, these techniques require expensive equipment, and they cannot monitor minute changes inside wafer-level vacuum cavities. Recent approaches for long-term monitoring of pressures use micromachined Pirani gauges, which provide an excellent solution for wafer-level sealed cavities as these gauges easily fit inside the sealed cavity and as they are fabricated in the same process together with MEMS structures to be vacuum sealed [5]–[11].

There are a number of micromachined Pirani gauges developed up to date [5]–[11] for monitoring pressures lower than 100 mTorr, which is a level of vacuum required for many MEMS devices. The first group of gauges are composed of a Cr/Pt resistor suspended on a dielectric membrane, such as the Pirani gauges presented by Shie *et al.* [5], Stark *et al.* [6], and the vertical design in the work by Chae *et al.* [7]. The second group of gauges consists of polysilicon or p^{++}-doped silicon microbridges, such as the vertical designs presented by Mastrangelo *et al.* [8], [9], Stark *et al.* [10], Mitchell *et al.* [11] and the lateral design presented by Chae *et al.* [7]. Except the process flow presented by Chae *et al.*, which includes a dissolved wafer process (DWP), the other processes do not include any thick structural layers. However, recently a number of other thick structural layer processes, such as silicon-on-glass (SOG) [12], [13], and silicon-on-insulator (SOI) processes [14]–[16], have been developed mostly for high performance inertial and resonant sensors, where their wafer-level vacuum packaging is essential for reducing the cost of the final products. For these processes, it is important to evaluate the vacuum level of the wafer level process in same wafer, which can be achieved with Pirani gauges suitable for these thick structural layer processes.

This paper presents Pirani vacuum gauges developed for two different fabrication processes with thick structural layers, namely, the DWP and SOG processes, where the approach can be adapted to SOI MEMS processes. To the best of authors' knowledge, the SOG Pirani gauge is the first gauge reported

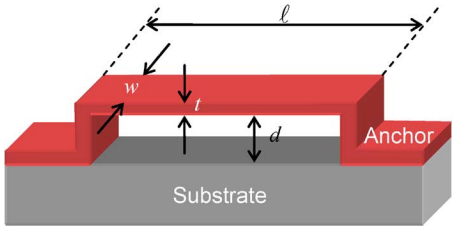

Fig. 1. The basic microbridge Pirani gauge structure, which is a suspended microbridge resistor with a value of R_o. This simplified structure can be used to extract the analytical modeling of Pirani gauges [8], [9].

in literature with such a thick (100 μm) structural layer. Each Pirani gauge design in this work have a meander-shaped suspended silicon resistor (heater) and two silicon islands (heat sinks) in the 2–3 μm proximity of the resistor, functioning as a dual-heat sink mechanism, as originally presented by Chae *et al.* [7]. The dual-heat sink approach enhances the sensitivity and dynamic range of the gauge compared to a single heat loss mechanism [7]. Moreover, the sensitivity and the dynamic range of the DWP and SOG Pirani gauges presented in this study are further improved by employing longer heaters than the structures in [7]. In addition, this study presents modeling of the Pirani gauges with thick structural layers, and first time, verifies that this modeling is consistent with the model developed for thin structural layers by Mastrangelo *et al.* [8], [9].

The Pirani gauges in this work are used to monitor the pressures of two different vacuum packages. The DWP Pirani gauge is used to detect the pressure of a wafer-level vacuum package, whereas the SOG Pirani is used the monitor the pressure inside a hybrid platform package vacuum-sealed using a projection welder.

II. Pirani Gauge Structures and Their Modeling

This section first presents the basic Pirani gauge structure and its model in order to explain the Pirani gauge structures developed in this study. Fig. 1 shows the basic Pirani gauge structure, which is a suspended microbridge resistor with a value of R_o. This simplified structure can be used to extract the analytical modeling of Pirani gauges [8], [9]. For a given current of I_b, the temperature of the resistor increases depending on the heat conducted through the gap between the Pirani gauge and the heat sink [5]–[11]. The amount of heat conducted through the gap is directly related to the interaction of the atoms in the surrounding gas, hence the pressure of the gas. The operation of the Pirani gauge is classified in three different pressure regimes. The temperature of the resistance does not change significantly at high pressures, since the density of gas atoms (pressure) and the resulting heat conduction through the gas are high. Therefore, the gauge is almost insensitive to the pressure changes in this pressure range. The temperature of the resistance changes significantly for moderate pressures, since the density of gas atoms, and hence, the heat conduction through the gas is lower. The resistance of the gauge increases as the pressure decreases in this region. Therefore, this pressure region is the dynamic range of the Pirani gauge. For relatively low pressures, the heat conduction through the solids such as anchors starts to dominate over the heat conduction through the gas, since the density of atoms gets lower. The gauge is almost insensitive to the pressure changes in this region.

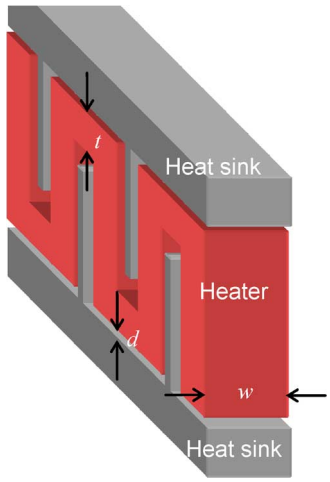

Fig. 2. The schematic drawing of the Pirani gauge designs with DHSs [7]. The gauges fabricated with the DWP and SOG processes have thicknesses (w) of 14 μm and 100 μm, respectively.

The analytical model derived by Mastrangelo *et al.* [8], [9] is used to numerically evaluate the operation of the Pirani gauge. The simple microbridge model in Fig. 1 is used to obtain the following expression for the microbridge resistance with a width of w, a length of λ, a thickness of t, and a gap of d between the bridge and the substrate (heat sink) [8], [9]

$$R_b = R_o\left[1+\frac{\delta\xi}{\varepsilon}\left(1-\frac{\tanh\sqrt{\varepsilon}\frac{\ell}{2}}{\sqrt{\varepsilon}\frac{\ell}{2}}\right)\right] \tag{1}$$

$$\delta = \frac{I_b^2 R_o}{\kappa_b wlt} \quad \varepsilon = \frac{\eta\kappa_{\rm gas}(P)}{\kappa_b td} - \delta\xi \tag{2}$$

where δ is the ohmic power generation, ε is the heat loss through the gas, I_b is the current applied to the bridge, η is a coefficient to include the fringing heat flux, and ξ is the temperature coefficient of resistance (TCR) of the bridge material. $\kappa_{\rm gas}(P)$ and κ_b are the thermal conductivities of the through the gas and through the beam, respectively [8], [9]. It is evident from (1) and (2) that passing a current of I_b through the microbridge changes the resistance due to the increase of the temperature across the microbridge. The average increase of the temperature across the microbridge can be found using the expression below

$$\Delta T_{\rm avg} = \left(\frac{R_b - R_o}{R_o}\right)\frac{1}{\xi}. \tag{3}$$

The thermal impedance of the gauge, which is used to evaluate the performance of the gauge at a specific pressure, is the slope of characteristics for the average temperature change, $\Delta T_{\rm avg}$, versus the power dissipated on the resistor. The sensitivity of a gauge is the slope of the thermal impedance versus the pressure [7].

The analysis and modeling presented above can be extended to the more complicated structures developed in this study. Fig. 2 shows the schematic drawing of the Pirani gauge designs presented in this work. The gauge uses the dual-heat sink structure, which is originally proposed by Chae *et al.* [7]. The dual heat sink (DHS) approach improves the sensitivity of the Pirani

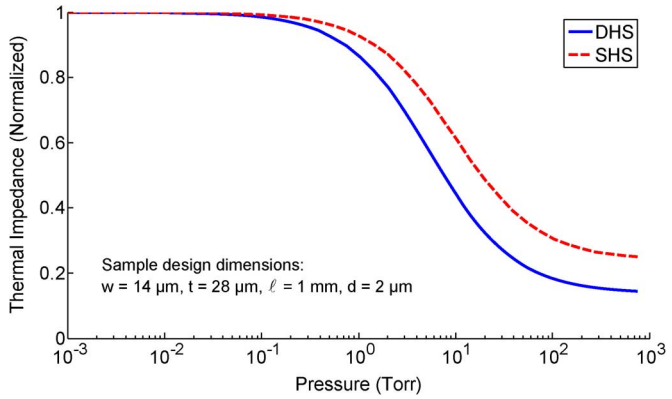

Fig. 3. Modeling results of the sample Pirani gauge structure with DHS and SHS approaches.

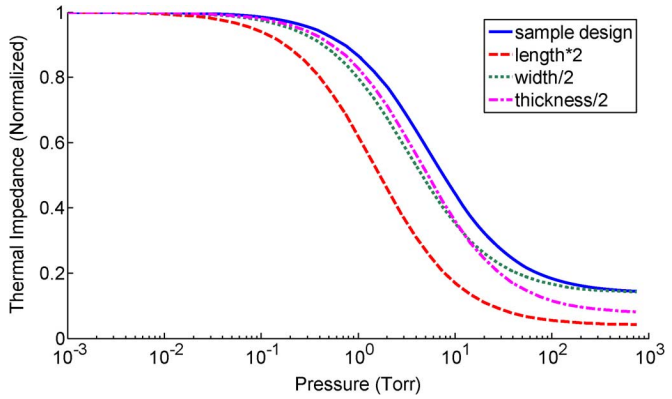

Fig. 4. A parametric analysis that demonstrates the effect of the physical dimensions on the performance of the sample design. The result of the sample designs are compared with twice the length, half of the width, and half of the thickness.

gauge as compared to the single heat sink (SHS) structure. The effect of DHSs is included by doubling the thermal conductivity through gas in (2).

Fig. 3 shows the modeling results of a sample design with DHS and SHS approaches with the physical dimensions given which is defined as the slope of the thermal impedance versus on the figure. The DHS approach yields higher sensitivity, pressure characteristics. Fig. 4 shows a parametric analysis that demonstrates the effect of the physical dimensions on the performance of the sample design. The analysis shows that decreasing the width and thickness and increasing the length of the heater shifts the characteristics towards lower pressures. The sensitivity also follows the same trend. Considering these, various Pirani gauges are designed for the DWP and SOG processes, the fabricated devices are measured, and the model is verified.

III. Design and Fabrication

Table I shows the physical dimensions and material properties of the DWP and SOG Pirani gauges that are developed in this study. The length of the gauges in this work is maximized to be approximately 40 mm by employing meanders in order to shift the dynamic ranges to the pressures lower than 100 mTorr. The limitation for the length is set by the standard cell and package layout size in METU process developed for the inertial sensors. The widths of the gauges are defined by the thicknesses of the

TABLE I
The Physical Dimensions and the Material Properties of the DWP and SOG Pirani Gauges That Are Developed in This Study

		DWP	SOG
Physical dimensions	w	14 μm	100 μm
	t	28 μm	28 μm
	ℓ	40 mm	40 mm
	d	2 μm	2 μm
Material properties	TCR, ξ	1500 ppm/°C [7]	1500 ppm/°C [7]
	κ_b	14.2 $W.K^{-1}.m^{-1}$ [18]	14.2 $W.K^{-1}.m^{-1}$ [18]
	Resistivity, ρ_o	7×10^{-6} Ω.m	5×10^{-5} Ω.m

structural layers in DWP (14 μm) and SOG (100 μm) processes. The thickness of the gauges is selected as 28 μm, which provides sufficient rigidity to the SOG Pirani gauge. It should be noted here that, the effect of the thickness of a Pirani gauge is not as significant as increasing the length considering the analysis presented in Fig. 4.

Fig. 5(a) and (b) shows the fabrication flows of the DWP and SOG processes, respectively. Both processes start with the preparation of the glass substrates on which the device anchors are defined by etching about 10 μm-depth recesses using pure hydrofluoric acid, where 100 Å/2000 Å-thick evaporated Cr/Au is the masking layer [Fig. 5(a)(i) and (b)(i)]. The recesses define the vertical distance between the heaters and the substrate, which is much larger compared to the lateral distance to the silicon islands in the 2–3 μm proximity of the heaters, therefore, the direct heat loss to the substrate can be neglected. After stripping Cr/Au masking layer for glass recesses, in order to have contacts to the Pirani gauge resistors, 100 Å/2000 Å-thick Cr/Au metallization is evaporated on glass substrates and patterned with a lithography followed by an etching process using commercial wet etchants [Fig. 5(a)(ii) and (b)(ii)]. The structural wafer in the DWP is a 500 μm-thick silicon wafer with a 14μm-thick heavily boron-doped layer on top of it [Fig. 5(a)(iii)]. The boron-doped side of the wafer is patterned with lithography and etched to have 20 μm deep trenches using Deep Reactive Ion Etching (DRIE) equipment, where the heater and heat sinks of the Pirani gauge are defined [Fig. 5(a)(iv)]. Next, the patterned side of structural wafer is anodically bonded to the glass substrate at 400 °C by applying a bias voltage of 1000 V at a pressure of 1.3 bar [Fig. 5(a)(v)].

The DWP is finalized by etching the undoped silicon wafer in ethylenediamine pyrocathecol (EDP) solution, until reaching the highly-doped structural silicon layer, at which the etch rate drops drastically [Fig. 5(a)(vi)] [15]. The structural wafer in the SOG process is a 100 μm-thick silicon wafer. 3000 Å-thick Al layer is evaporated on 100 μm-thick silicon wafer and patterned as the shield metallization in order to avoid ion damaging and overheating problems during DRIE of the silicon wafer [Fig. 5(b)(iii) and (b)(iv)] [12]. The surface of the structural wafer with shield metallization is anodically bonded to the glass substrate using the same recipe given above [Fig. 5(b)(v)]. The SOG process is finalized by DRIE of the silicon wafer and selective removal of the shield metallization using commercially available aluminum etchant [Fig. 5(b)(vi)].

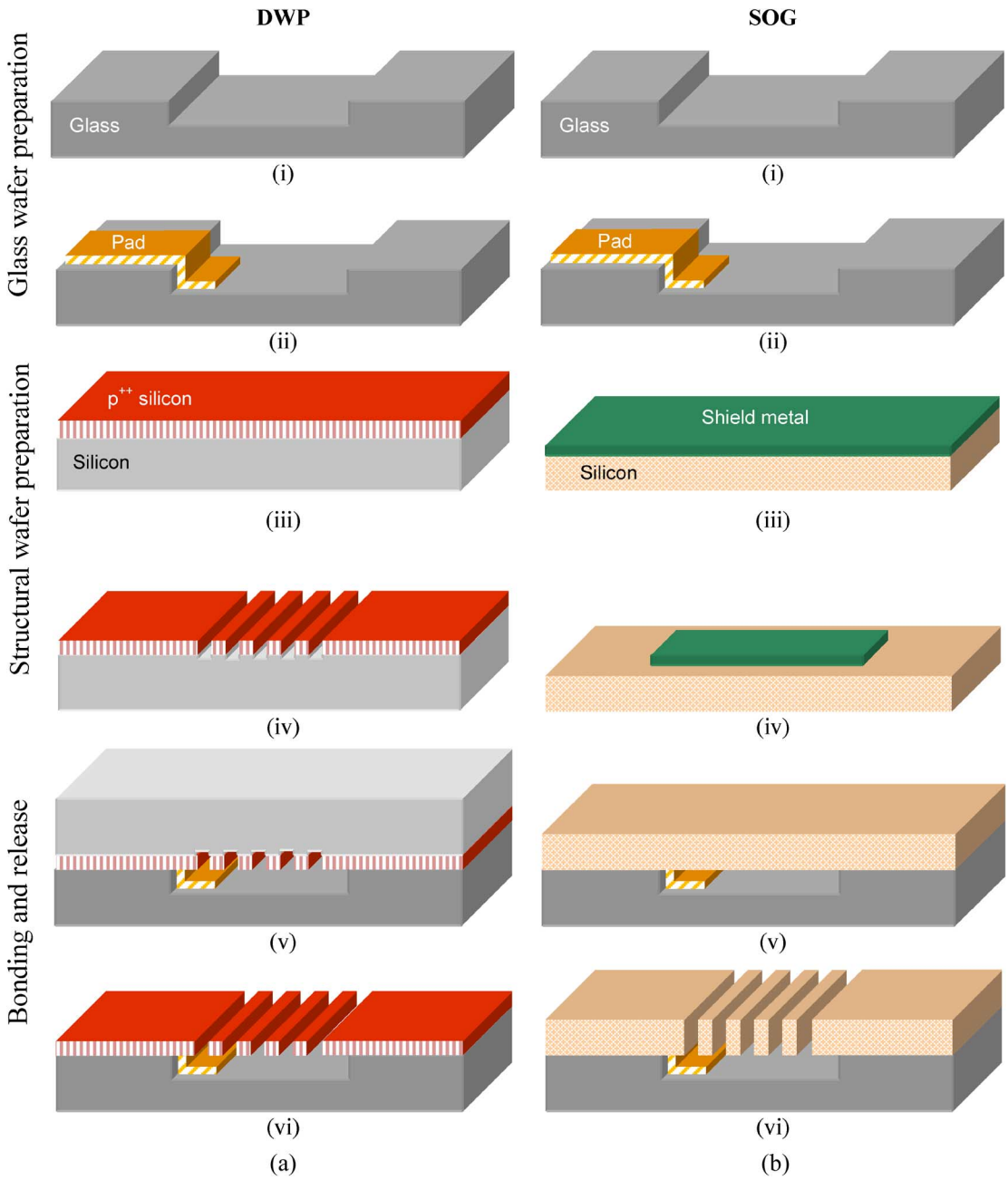

Fig. 5. Fabrication process flows: (a) DWP and (b) SOG processes.

Fig. 6 shows the SEM photographs of these Pirani gauges, where the buckling of the heater in the DWP Pirani gauge is observed due to internal stress of the highly boron-doped structural layer. The buckling reduces the device performance as the thermal impedance reduces due to the extra heat conduction to the substrate. The buckling problem does not occur in the SOG process, as there is no internal stress in the structural silicon layer and as the structural layer is very thick compared to the DWP process. The measurement results of the fabricated Pirani gauges are presented in the next section.

IV. Measurement Results

The Pirani gauges are measured using the four-point probe method, where a current I_b is applied to the gauge and the voltage drop V_b is measured across the same terminals [6], [7], [10], [11]. Fig. 7 shows the measurement setup used to characterize the Pirani gauges. The current is supplied via the Keithley 224 current source and the voltage is measured via the HP 34401A digital multimeter. Vacuum pressures are achieved using a roughing pump, where a needle valve is attached between the pump and the chamber in order to control the pressure. The temperature change is extracted from (3), and the power is found from the measured voltages and currents [7]. The current is increased until the temperature change reaches to about 35 °C keeping the pressure same. Fig. 8 shows the temperature change versus applied power characteristics of the DWP Pirani gauge. The slope of the linearly fitted curves in the temperature change versus the power provides the thermal

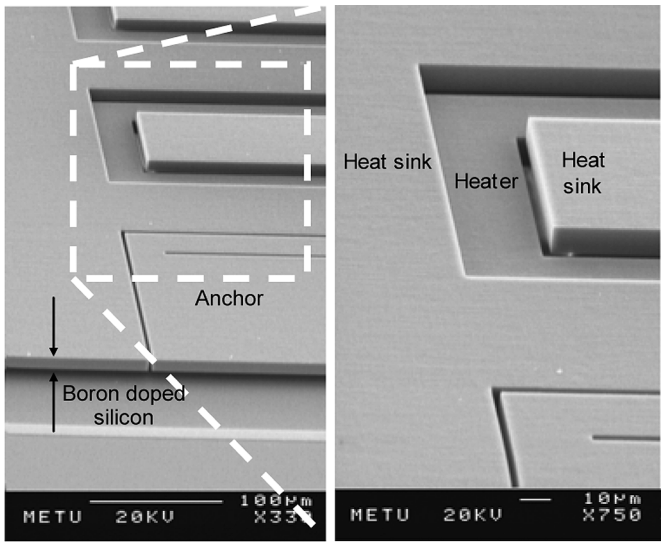

(a)

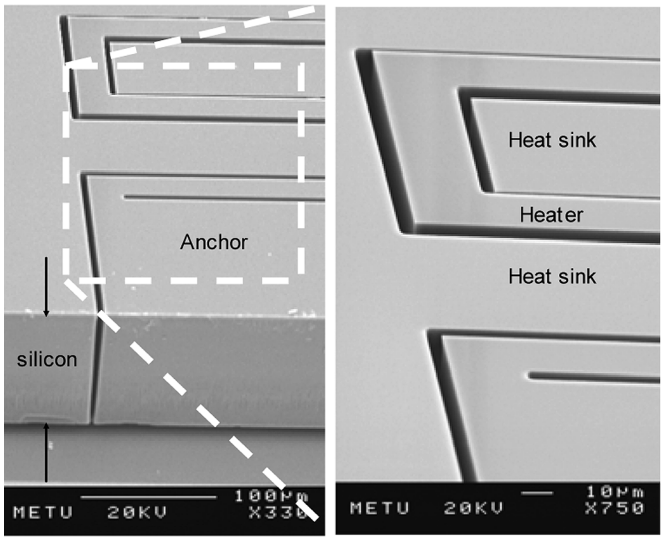

(b)

Fig. 6. The SEM photographs of the Pirani gauges: (a) DWP Pirani gauge and (b) SOG Pirani gauge.

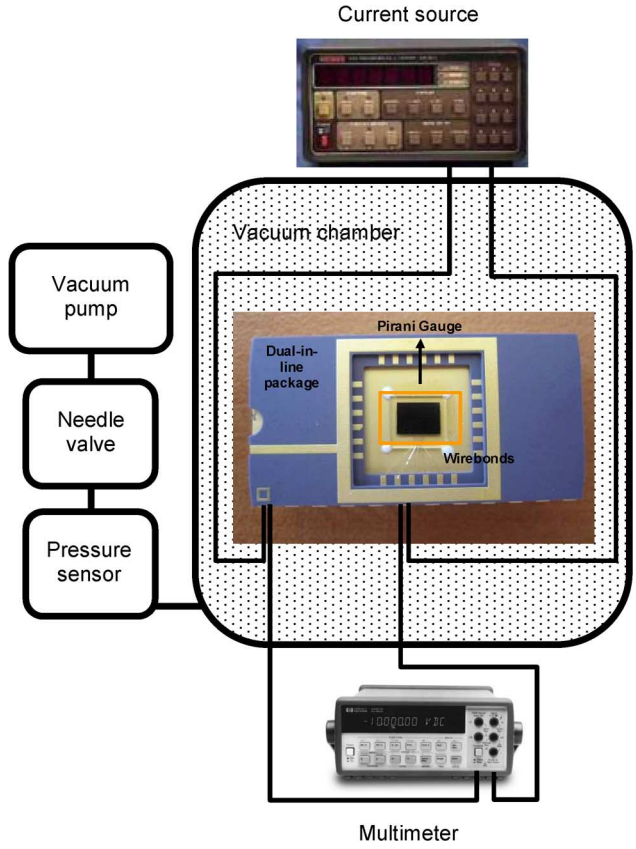

Fig. 7. The measurement setup used to characterize the Pirani gauges.

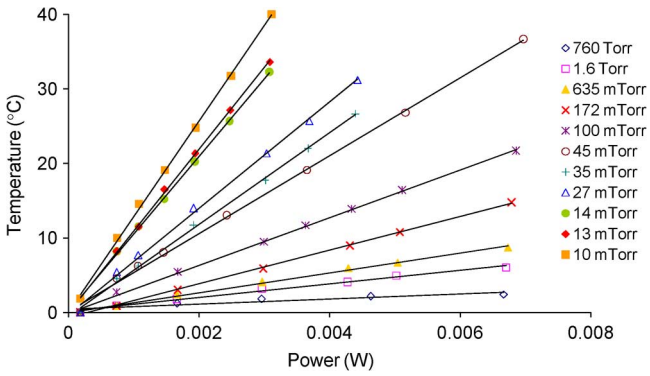

Fig. 8. The temperature change versus applied power characteristics of the DWP Pirani gauge. The slope of the characteristics for each pressure gives the thermal impedance value.

impedance for the corresponding pressure. The same method is also applied to the SOG Pirani gauge. Fig. 9 shows the thermal impedance versus pressure characteristics of the DWP and SOG Pirani gauges. The DWP Pirani gauge is able to measure lower pressures with a higher sensitivity compared to the SOG Pirani gauge. The DWP Pirani gauge shows a sensitivity of 4.2×10^4 (K/W)/Torr in a dynamic range of 10–2000 mTorr. It should be noted here that the measured dynamic range is limited by the available vacuum pump, which allows reaching pressures down to 10 mTorr. The actual dynamic range of the DWP Pirani gauge is larger, as will be shown with the analytical modeling below. The SOG Pirani gauge shows a lower sensitivity of 3.8×10^3(K/W)/Torr in a dynamic range 50–5000 mTorr, which is consistent with the results given in Fig. 4; however, its mechanical rigidity and reliability against the residual stress in the suspended silicon layer are superior compared to the DWP Pirani gauges due to the 100 μm-thick silicon heater and heat sinks used in the SOG process.

In order to define the uncertainty in the thermal impedance measurements, the Pirani gauges are measured ten times with 5 min intervals at 100 mTorr. Fig. 10 shows the variance of the thermal impedances of the gauges at 100 mTorr. The plot indicates that the thermal impedance of the DWP Pirani gauge has 130 K/W standard deviation with a mean value of 3002 K/W, which corresponds to 6 mTorr uncertainty around 100 mTorr. Applying the similar analysis, it is found that the SOG Pirani gauge shows 13 mTorr uncertainty around 100 mTorr.

Table II summarizes the processes and the dynamic ranges of the Pirani gauges in literature and in this work. As compared

TABLE II
A SUMMARY OF SOME OF THE PIRANI GAUGE DESIGNS IN LITERATURE AND IN THIS WORK THAT CAN MEASURE PRESSURES LOWER THAN 100 mTorr

Researcher	Type of the gauge	Process summary	Pressure range
Shie *et. al.* [5]	Cr/Pt resistor on a dielectric membrane	Bulk micromachining	10^{-7}–1 Torr*
Stark *et. al.* [6]	Cr/Pt resistor on a dielectric membrane	Surface micromachining with polysilicon sacrificial layer	10^{-3}–10 Torr
Chae *et. al* [7]	Cr/Pt resistor on a dielectric membrane anchored to p^{++} silicon	Surface micromachining with polysilicon sacrificial layer	2×10^{-2}–2 Torr
Mastrangelo and Muller [8], [9]	Polysilicon microbridge	Surface micromachining with n^{+} polysilicon sacrificial layers	7.5×10^{-2}–75 Torr
Stark *et. al.* [10]	Polysilicon microbridge	Surface micromachining with silicon dioxide sacrificial layer	10^{-2}–100 Torr
Mitchel *et. al.* [11]	Polysilicon microbridge	Surface micromachining with silicon dioxide sacrificial layer	5×10^{-2}–760 Torr
Chae *et. al* [7]	p^{++} silicon coil microbridge	Dissolved wafer process	5×10^{-2}–5 Torr
This work	p^{++} silicon coil microbridge	Dissolved wafer process	10^{-2}–2 Torr
This work	100 μm-thick silicon coil microbridge	Silicon-on-glass process	5×10^{-2}–5 Torr

* The dynamic range is enhanced with the use of constant-temperature circuit, thermoelectric stabilization, and an integrated reference resistor.

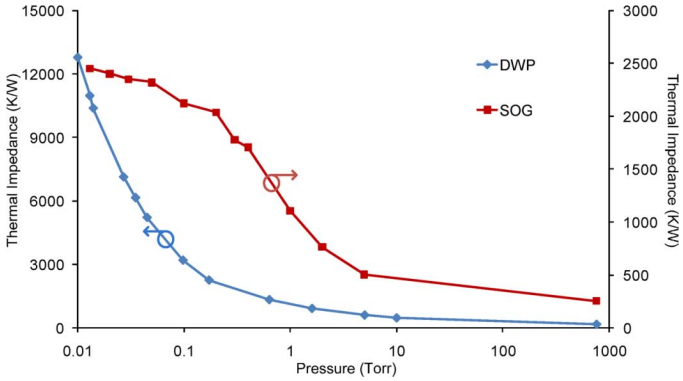

Fig. 9. The thermal impedances versus pressure characteristics of the DWP and SOG Pirani gauges.

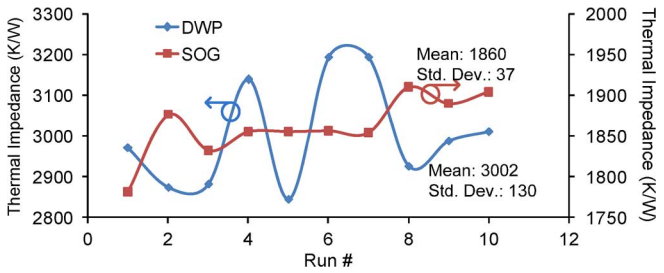

Fig. 10. The variance of the thermal impedances of the gauges at 100 mTorr. The DWP Pirani gauge has a mean thermal impedance of 3002 K/W with a standard deviation of 130 K/W. The SOG Pirani gauge has a mean thermal impedance of 1860 K/W with a standard deviation of 37 K/W.

with the ones in literature, the gauges presented in this work provide similar dynamic ranges with such thick structural layers, and therefore, they can directly and easily be used to monitor the performance of wafer-level vacuum packaging of thick structural MEMS processes, such as DWP and SOG as well as SOI MEMS.

Fig. 11 shows the photograph of the wafer-level packaged MEMS devices fabricated using the DWP at METU. The wafer-level packaging technique employs a silicon cap with a thin-film getter, bonded to the device wafer with the aid of glass frit bonding [2]. The getters and glass frits of the silicon cap are coated by Nanogetters, Inc. [19]. The DWP Pirani

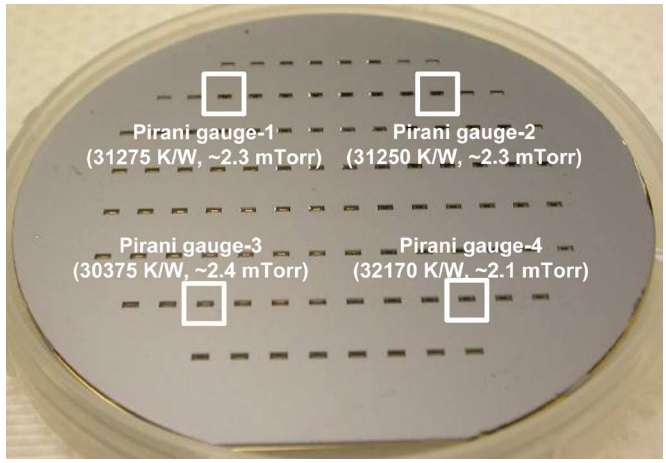

Fig. 11. The wafer-level packaged devices fabricated using DWP at METU. The locations and measured thermal impedances of the Pirani gauges are indicated on the photograph.

gauges are placed at the corners of the wafer in order to predict the pressures inside the microcavities. The packaged Pirani gauges are tested under probe station, and thermal impedances ranging from 30,375 to 32,170 K/W are extracted. Fig. 12 shows the results of the analytical model, which is fitted to the previously measured values in the vacuum chamber. The thermal impedance values obtained from the model is divided by a correction factor, k of 12.5 in order to match to the measured values (fringing heat flux coefficient, η in (2) is equal to unity). The need for correction factor is a result of the buckling of the heater and the assumptions in the model and material properties [11]. Considering the uncertainty measurements at 100 mTorr, the gauge has an uncertainty of 0.3 mTorr around 2.4 mTorr for a standard deviation of 1300 K/W, which is found by scaling the measured standard deviation at 100 mTorr. The SOG Pirani gauge is used to measure the pressure inside a hybrid platform package (without any getter), on which the cover is welded under vacuum using a projection welder. The measured thermal impedance of the packaged SOG devices is 922 K/W, which corresponds to a pressure of 1400 mTorr. The uncertainty is 50 mTorr at 1400 mTorr for a standard deviation of 18 K/W at 1400 mTorr, which is found by scaling the

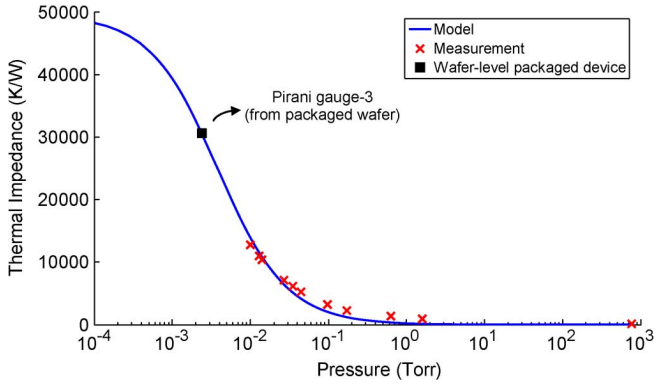

Fig. 12. The results of the analytical model for the DWP Pirani gauge, which is fitted to the previously measured values in the vacuum chamber. These results are used to predict the pressure inside the microcavities of a wafer-level vacuum package.

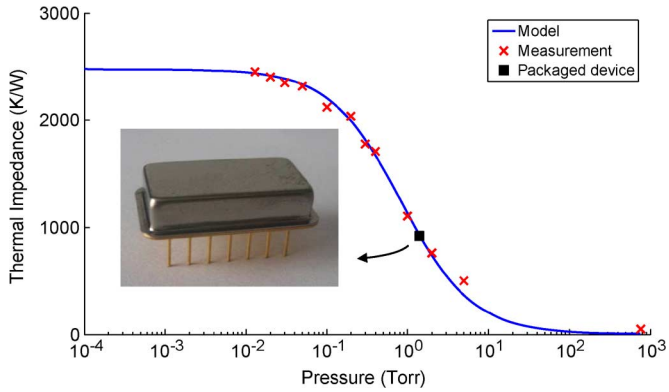

Fig. 13. The results of the analytical model for the SOG Pirani gauge, which is fitted to the previously measured values in the vacuum chamber. These results are used to predict the pressure inside the vacuum-sealed hybrid platform package.

measured standard deviation at 100 mTorr. Fig. 13 shows the results of the analytical model which is fitted to the measured thermal impedances of the SOG Pirani gauge in the vacuum chamber. It should be noted here that the correction factor k and fringing heat flux coefficient η are 34 and 0.13, respectively. The high correction factor for the SOG Pirani gauge is required to match the measurement results with the model, as the heat distribution in a meander-shaped thick structural layer is not same as that of straight thin structural layers. The accurate modeling of meander-shaped Pirani gauge structures requires a parametric study on fabricated Pirani gauges with different physical dimensions, which is considered in the framework of a future study.

ACKNOWLEDGMENT

The authors would like to thank O. Pasin for her help during the initial design and modeling and I. Ender Ocak and Y. Temiz for their help during the initial tests. They also would like to thank the METU-MET staff, particularly, O. Sevket Akar for their support in the fabrication.

REFERENCES

[1] J. Chae, J. M. Giachino, and K. Najafi, "Fabrication and characterization of a wafer-level MEMS vacuum package with vertical feedthroughs," *J. Microelectromech. Syst.*, vol. 17, no. 1, pp. 193–2000, Feb. 2008.

[2] D. Sparks, N. Najafi, and S. Ansari, "Chip-level vacuum packaging of micromachines using nanogetters," *IEEE Trans. Adv. Packag.*, vol. 26, no. 3, pp. 277–282, Aug. 2003.

[3] Y. Cheng, W. Hsu, K. Najafi, C. T. Nguyen, and L. Lin, "Vacuum packaging technology using localized aluminum/silicon-to-glass bonding," *J. Microelectromech. Syst.*, vol. 11, no. 5, pp. 556–565, Oct. 2002.

[4] D. Sparks, G. Queen, R. Weston, G. Woodward, M. Putty, L. Jordan, S. Zarabadi, and K. Jayakar, "Wafer-to-wafer bonding of nonplanarized MEMS surfaces using solder," *J. Micromech. Microeng.*, vol. 11, pp. 630–634, 2001.

[5] J. Shie, B. C. S. Chou, and Y. Chen, "High performance Pirani vacuum gauge," *J. Vac. Sci. Technol. A, Vac. Surf. Films*, vol. 13, no. 6, pp. 2972–2979, Nov. 1995.

[6] B. H. Stark, Y. Mei, C. Zhang, and K. Najafi, "A doubly anchored surface micromachined Pirani gauge for vacuum package characterization," in *Proc. IEEE 16th Annu. Int. Conf. Micro Electro Mech. Syst.*, Jan. 19–23, 2003, pp. 506–509.

[7] J. Chae, B. H. Stark, and K. Najafi, "A micromachined Pirani gauge with dual heat sinks," *IEEE Trans. Adv. Packag.*, vol. 28, no. 4, pp. 619–625, Nov. 2005.

[8] C. H. Mastrangelo and R. S. Muller, "Microfabricated thermal absolute pressure sensor with on-chip digital front-end processor," *IEEE J. Solid-State Circuits*, vol. 26, no. 12, pp. 1998–2007, Dec. 1991.

[9] C. H. Mastrangelo and R. S. Muller, "Fabrication and performance of a fully integrated μ-Pirani pressure gauge with digital readout," in *Proc. Int. Conf. Solid-State Sens. Actuators*, Jun. 24–28, 1991, pp. 245–248.

[10] B. H. Stark, J. Chae, A. Kuo, A. Oliver, and K. Najafi, "A high performance surface-micromachined Pirani gauge in SUMMIT V," in *Proc. 18th IEEE Int. Conf. Micro Electro Mech. Syst.*, Jan. 30–Feb. 3 2005, pp. 295–298.

[11] J. Mitchell, G. R. Lahiji, and K. Najafi, "An improved performance poly-Si Pirani vacuum gauge using heat-distributing structural supports," *J. Microelectromech. Syst.*, vol. 17, no. 1, pp. 93–102, Feb. 2008.

[12] J. Chae, H. Kulah, and K. Najafi, "A hybrid Silicon-on-Glass (SOG) lateral micro-accelerometer with CMOS readout circuitry," in *Proc. IEEE MicroElectro Mech. Syst. Workshop (MEMS'02)*, Las Vegas, NV, Jan. 2002, pp. 623–626.

[13] J. Chae, H. Kulah, and K. Najafi, "A CMOS-compatible high aspect ratio silicon-on-glass in-plane micro-accelerometer," *J. Micromech. Microeng.*, vol. 15, pp. 336–345, 2005.

[14] S. E. Alper, K. Azgin, and T. Akin, "A high-performance silicon-on-insulator MEMS gyroscope operating at atmospheric pressure," *Sens. Actuators A*, vol. 135/1, pp. 34–42, Mar. 2007.

[15] [Online]. Available: http://www.memscapinc.com/en_mumps.html

[16] [Online]. Available: http://www.tronics.eu/mems-technology/soi-mems-drie-bulk-micromachining.html

[17] Y. B. Gianchandani and K. Najafi, "A bulk silicon dissolved wafer process for microelectromechanical devices," *J. Microelectromech. Syst.*, vol. 1, no. 2, pp. 77–85, Jun. 1992.

[18] A. Jacguot, W. L. Liu, G. Chen, J.-P. Fleurial, A. Dauscher, and B. Lenoir, "Figure-of-merit and emissivity measurement of fine-grained polycrystalline silicon thin films," in *Proc. 21st ICT*, Aug. 25–29, 2002, pp. 118–121.

[19] [Online]. Available: http://www.nanogetters.com/

Ebru Sagiroglu Topalli was born in Iskenderun, Turkey, in 1978. She received the B.S. and M.S. degrees (high honors) in engineering physics from Ankara University, Ankara, Turkey, in 1999 and 2001, respectively. She is currently working towards the Ph.D. degree at the Department of Engineering Physic, Ankara University.

From 1999 to 2004, she was a Research Engineer at the Department of Engineering Physic, Ankara University. She received the graduate fellowship provided by the Scientific and Technical Research Council of Turkey (TUBITAK) between 2000 and 2004. Since 2004, she has been employed as a Research Scientist in the Microelectronics Technologies Facility, Middle East Technical University (METU-MET). Her major research interests include development of microfabrication and packaging technologies for MEMS inertial sensors.

Kagan Topalli (S'99–M'08) was born in Eskisehir, Turkey, in 1979. He received the B.S. and Ph.D. degrees in electrical and electronics engineering from Middle East Technical University (METU), Ankara, Turkey, in 2001 and 2007, respectively.

From 2001 to 2007, he was a Research Assistant at METU, Department of Electrical and Electronics Engineering. He is currently a Senior Research Scientist in the Department of Electrical and Electronics Engineering. His major research interests include development, characterization, and integration of novel RF MEMS structures such as switches, phase shifters, and impedance tuners for RF front ends at microwave and milimeter-wave, reconfigurable antennas, phased arrays, microwave packaging, and microfabrication technologies.

Dr. Topalli received the METU Thesis of the Year Award in 2007 for his Ph.D. dissertation, which was awarded by Prof. Mustafa N. Parlar Education and Research Foundation.

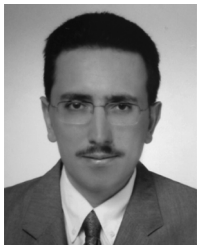

Said Emre Alper was born in Ankara, Turkey, in 1976. He received the B.S., M.S., and Ph.D. degrees in electrical and electronics engineering (with high honors) from Middle East Technical University (METU), Ankara, in 1998, 2000, and 2005, respectively.

From 1998 to 2005, he was a Research Assistant with the MEMS-VLSI Research Group, Department of Electrical and Electronics Engineering, METU, where he has been a Senior Research Scientist since 2006. His major research interests include capacitive MEMS inertial sensors, capacitive interface circuits, analog closed-loop control, microfabrication technologies, and packaging.

Dr. Alper received the METU Thesis of the Year Award in 2000 and 2005 for his M.Sc. thesis and Ph.D. dissertation, respectively, which were awarded by the Prof. Mustafa N. Parlar Education and Research Foundation. He is the first author of the symmetric and decoupled gyroscope design, which won the first prize award in the operational designs category of the International Design Contest " organized by Design, Automation, and Test (DATE) Conference in Europe and CMP in March 2001. He is also the first author of the tactical-grade symmetrical and decoupled microgyroscope design, which won the third-prize award, among 132 MEMS designs from 24 countries and 25 states across the U.S., in the international 3-D MEMS Design Challenge organized by MEMGEN Corporation (currently,Microfabrica, Inc.) in June 2003.

Tulay Serin was born in Rize, Turkey, in 1954. She received the B.S., M.S., and Ph.D. degrees in engineering physics from Ankara University, Ankara, Turkey, in 1977, 1983, and 1988, respectively.

From 1979 to 1988, she was a Research Assistant at the Department of Engineering Physics, Ankara University. Since 1988, 1993, and 1998, she has been employed as an Assistant Professor, Associate Professor, and Professor, respectively, in the Department of Engineering Physics, Ankara University. Her major research interests include the investigation of electronic properties of Schottky and pin diode structures composed of various thin layers such as amorphous silicon, silicon, and germanium.

Tayfun Akin (S'90–M'97) was born in Van, Turkey, in 1966. He received the B.S. degree in electrical engineering (high honors) from Middle East Technical University, Ankara, Turkey, in 1987, and went to the U.S. in 1987 for his graduate studies with a graduate fellowship provided by NATO Science Scholarship Program through TUBITAK. He received the M.S. degree in 1989 and the Ph.D. degree in 1994 in electrical engineering, both from the University of Michigan, Ann Arbor.

Since 1995, 1998, and 2004, he has been employed as an Assistant Professor, Associate Professor, and Professor, respectively, in the Department of Electrical and Electronics Engineering at Middle East Technical University. He is also the Director of METU-MEMS Research Center, which has a 1300m^2 clean room area for MEMS process and testing. His research interests include microelectromechanical systems (MEMS), microsystems technologies, infrared detectors and readout circuits, silicon-based integrated sensors and transducers, and analog and digital integrated circuit design.

Dr. Akin has served in various MEMS, Eurosensors, and Transducers Conferences as a Technical Program Committee Member. He was the Co-Chair of the 19th IEEE International Conference of Micro Electro Mechanical Systems (MEMS 2006) held in Istanbul. He is the winner of the First Prize in Experienced Analog/Digital Mixed-Signal Design Category at the 1994 Student VLSI Circuit Design Contest organized and sponsored by Mentor Graphics, Texas Instruments, Hewlett-Packard, Sun Microsystems, and Electronic Design Magazine. He is the coauthor of the symmetric and decoupled gyroscope project which won the First Prize Award in the operational designs category of the international design contest organized by DATE Conference and CMP in March 2001. He is also the coauthor of the gyroscope project which won the Third Prize Award of 3-D MEMS Design Challenge organized by MEMGen Corporation (currently, Microfabrica).